A Review on Wetting and Water Condensation - Perspectives for CO_2 Condensation

Ingrid Snustad[a,*], Ingeborg T Røe[b], Amy Brunsvold[b], Åsmund Ervik[b], Jianying He[a], Zhiliang Zhang[a]

[a] *Faculty of Engineering, Department of Structural Engineering, Norwegian University of Science and Technology Høgskoleringen 6, NTNU Faculty of Engineering 7491 Trondheim, Norway*
[b] *SINTEF Energy Research*

Abstract

Mitigation of CO_2 emissions is an increasingly important mean for reducing global warming. Liquefaction of CO_2 is sometimes a necessary, but energy intensive step in the carbon capture, transport and storage chain and a reduction in energy consumption is therefore important. This review identifies possible materials and surface structures for promoting dropwise CO_2 condensation with applications in heat exchange technologies. Research on superhydrophobic and ~~superlyophobic~~ superomniphobic surfaces promoting dropwise condensation constitutes the basis for the qualitative analysis of possible surfaces promoting dropwise CO_2 condensation. The review is divided into three main parts: 1) An overview of recent research on superhydrophobicity and promotion of dropwise condensation of water, 2) An overview of recent research on ~~superlyophobicity~~ superomniphobicity and dropwise condensation of low surface tension substances, and 3) Suggested materials and surface structures for dropwise CO_2 condensation based on the two first parts.

Keywords: CCS, dropwise condensation, nanostructured surfaces, superhydrophobicity, ~~superlyophobicity~~ superomniphobicity

*Corresponding author
Email address: ingrid.snustad@ntnu.no (Ingrid Snustad)

1. Introduction

~~To combat anthropogenic global warming, large scale, world wide CO_2~~Condensation of vapor is a necessary and energy consuming step in several industrial processes, such as HVAC systems [1], waste heat recovery [2], LNG production [3] and for potential CO_2 ~~capture, transport and storage (CCS) must become a reality . Liquefaction of gaseous CO_2 has become an increasingly important field as the demand for improved and more energy efficient CCS increases. The liquefaction is an important part of several processes within the CCS chain, e.g. for post processing after capture technologies such as oxyfuel combustion, and as a necessary step for ship transport .~~

capture [4], and ship transportation of CO_2 [5]. The liquefaction of any vapor involves condensation on a surface where heat is transferred from the vapor to the surface. Increasing the heat transfer rate will therefore increase the liquefaction efficiency of the vapor. Through extensive research on condensation, it is apparent that with dropwise condensation the heat transfer rate could be increased by an order of magnitude [6, 7, 8, 9]. Although the condensation of other gases than water have attracted more attention over the past decade[10, 11], the mechanism of dropwise condensation of water vapor is still ~~better understood. This review article therefore~~ best understood.

This review gives an overview of the research on the parameters affecting and controlling dropwise condensation of water vapor. ~~Further, in order to understand the mechanisms necessary for increasing the liquefaction efficiency of CO_2~~Dropwise condensation is a cyclic process including initial nucleation, growth, and coalescence of droplets, followed by droplet removal. In this paper we focus on the properties governing the surface adhesion of droplets after nucleation and initial coalscence. Further, we will compare these parameters with those found to control the condensation of low surface tension substances (commonly non-polar substances such as ethanol, hexadecane etc). ~~Based on the research on water and non-polar substances, we will qualitatively determine the~~

parameters that control the Surfaces that promote dropwise condensation of low surface tension fluids will be examined and the important properties discussed. A small discussion on condensation of CO_2 on a functionalized surface . This will create a new path of research, as dropwise condensation of is included at the end of the review. CO_2 is a very low surface tension fluid ($\approx 4\,\mathrm{mN\,m^{-1}}$ at room temperature), and is interesting both for academic and environmental purposes. Liquefaction of gaseous CO_2 is previously not investigated. an important field since improved and more energy efficient carbon capture, transport and storage (CCS) is necessary for combating anthropogenic global warming.

To fully understand the mechanisms affecting and controlling the condensation, we will , however, first give a brief introduction to the parameters affecting the shape and morphology of static droplets on a surface.

2. Hydrophobicity, Contact Angles and Wetting Modes

Hydrophobicity, contact angles and wetting modes are underlying phenomena for dropwise condensation. A surface is labelled hydrophobic when it is repellent towards water, i.e. the contact angle (CA), θ, of water on the surface is larger than 90°. Various terms are used when surfaces are repellent towards other liquids. These are oleophobic if oil repellent, amphiphobic if repellent towards oil and water, and omniphobic if repellent towards polar and apolar substances and lyophobic if repellent towards any liquid. The same holds for -philic surfaces, which are attractive to the same compounds.

For a surface to be termed with the prefix super- (such as superhydrophobic), the surface must exhibit $\theta \geq 150°$ and contact angle hysteresis (CAH) $\Delta\theta \leq 10°$. CAH is defined as the difference between the receding and the advancing CA.

The -phobic and -philic terms and the super- term are used somewhat inconsequently in the literature, and often refer to the same types of surfaces. In this review, the definitions above will be used.

This Section explains the above mentioned phenomena and goes through the most important Equations describing the governing mechanisms.

2.1. Hydrophobicity and Young Contact Angle

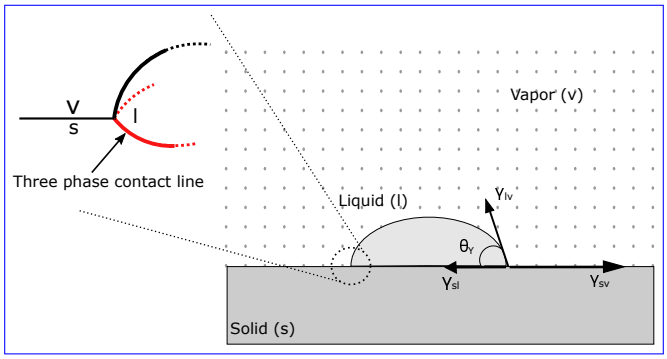

Figure 1: Young contact angle, θ_Y, at one point on the three phase contact line (shown in inset), and the surface tensions, γ_{ij}, between the different phases.

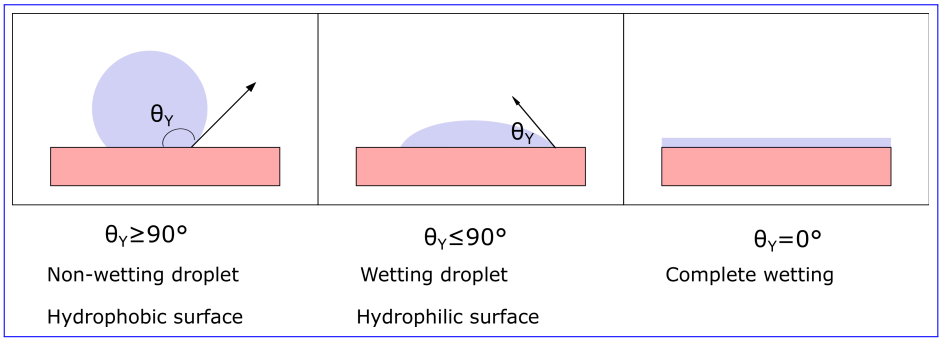

Figure 2: Wetting modes of water on different surfaces described by the contact angle θ. Figure adapted from Hiemenz, P.C. and Rjagopalan, R. (1997)[12]

As water droplets form on surfaces that repel water, hydrophobic surfaces have normally been utilized to achieve dropwise water condensation. The hydrophilicity and hydrophobicity of a material are characterized by the Young contact angle, θ_Y, which is the liquid-solid contact angle on a flat surface defined in Figure 1. The relation between θ_Y and the wetting modes is shown in Figure 2. A surface is said to be hydrophobic when $\theta_Y \geq 90°$. This is, however, insufficient for sustained dropwise condensation since coalescence of droplets eventually leads to film formation. To avoid extensive coalescence, the droplet

mobility must be high enough to ensure sustained self-removal of droplets from the surface. High droplet mobility results from a low contact angle hysteresis (CAH), $\Delta\theta$, defined in Figure 3. Surfaces having $\theta_Y \geq 150°$ and $\Delta\theta \leq 10°$ towards water are called superhydrophobic surfaces, on which dropwise condensation is usually achievable.

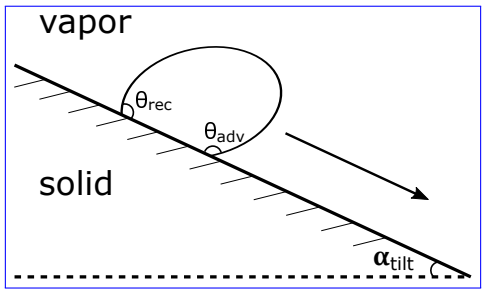

Figure 3: Advancing, θ_{adv}, and receding, θ_{rec}, contact angles on a tilted surface with tilting angle α_{tilt}. The CAH is $\Delta\theta = \theta_{adv} - \theta_{rec}$

2.2. Superhydrophobicity, and Cassie-Baxter and Wenzel state

While the hydrophobicity of a surface is determined by the surface chemistry, the superhydrophobicity of a surface cannot be manipulated through the surface chemistry alone. To our knowledge, there are no flat surfaces exhibiting $\theta > 120°$[13], and hence, no flat superhydrophobic surfaces. However, an apparent contact angle above 120° is attainable by introducing surface roughness. According to the Wenzel equation[14], the apparent equilibrium contact angle, θ^*, is a function of the roughness factor, $r = \frac{actual\ surface\ area}{apparent\ surface\ area}$, and the Young contact angle, θ_Y:

$$cos\,\theta^* = r\,cos\,\theta_Y\,. \tag{1}$$

Since $r \geq 1$, Equation (1) shows that $\theta^* \geq \theta_Y$ for $\theta_Y \geq 90°$. However, Equation (1) is only valid for droplets where the structure under the droplet is fully wetted as illustrated in Figure 4(a). In the case where vapor is trapped between the droplet and the surface as shown in Figure 4(b), the droplet is in

the Cassie-Baxter state[1] and the Cassie-Baxter equation is valid[15]:

$$cos\,\theta^* = r_f\, f_s\, cos\,\theta_Y + f_s - 1, \tag{2}$$

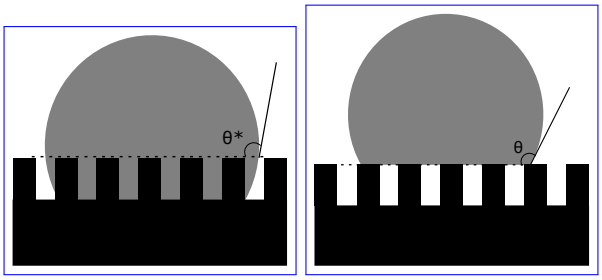

(a) The Wenzel state (b) The Cassie-Baxter state

Figure 4: Sketch of droplets in different states on a rough surface.

where $r_f = \frac{actual\ wetted\ surface\ area}{apparent\ wetted\ surface\ area}$ and $f_s = \frac{apparent\ wetted\ solid\ surface\ area}{apparent\ solid\ surface\ area}$, i.e. the fraction of the liquid droplet's footprint in contact with the solid, or solid fraction. In the situation where the droplet is "floating" completely on top of the surface structure, $r_f = 1$, and Equation (2) reduces to:

$$cos\,\theta^* = f_s\, cos\,\theta_Y + f_s - 1. \tag{3}$$

In the other extreme situation where the rough surface under the droplet is fully wetted, $f_s = 1$ and $r_f = r$ and Equation (2) reduces to Equation (1)[2]. To achieve a contact angle above 90° on a rough surface, it is, according to the Cassie equation, necessary to have $f_s < \frac{1}{1+r_f\cos(\theta_Y)}$. In Figure 5, contact angles for droplets with ~~θ_Y~~ $\theta_Y = 50°$ and with $r_f = 1$ with varying f_s is shown. A solid fraction less than 0.6 is sufficient to achieve non-wetting behaviour, while f_s less than ~~0.07~~ 0.08 is necessary for superhydrophobicity ($\theta_{CB} > 150°$).

Since droplets in the Wenzel state completely wet the surface under the droplet, the state is associated with high contact line pinning and thus low

[1] From now on called the Cassie state

[2] Even though we have been talking about superhydrophobicity here, it is worth to note that Equation (1) and (2) are valid for the apparent equilibrium contact angle of any liquid

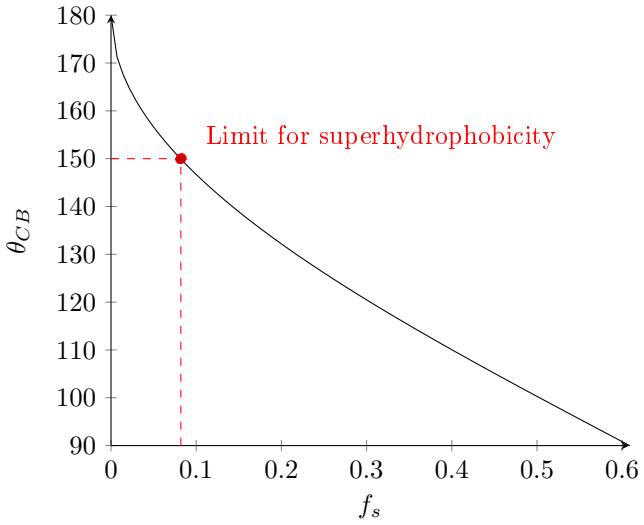

Figure 5: Cassie contact angle, θ_{CB} in degrees, for varying solid fractions, f_s, for a Young contact angle of 50°.

droplet mobility. The contact line is the line where vapor, liquid and solid are in contact (see Figure 1). Because the motivation is to induce dropwise condensation, the mobile Cassie state is desirable. However, it is challenging to determine when the droplet will stabilize in the Cassie state instead of the Wenzel state since neither Equation (1) nor (3) describes the stability of the states. The only thing we may extract from Equation (1) and (3) is the critical equlilibrium Young contact angle, $\theta_{Y\,crit}$, for which the droplet transitions from the Cassie to the Wenzel state. By equating Equation (1) and (3), we find $\theta_{Y\,crit} \geq 90°$, i.e. that the Wenzel to Cassie transition occurs above 90°. Although Equation (3) indicates that $\theta^* > \theta_Y$ for $\theta_Y < 90°$ is possible, the $\theta_{Y\,crit}$ reaffirms that a thermodynamically stable Cassie state can not exist for $\theta_Y < 90°$. This does not, however, mean that droplets always form in the Cassie state for $\theta_Y \geq 90°$. On the contrary, the Wenzel state is often observed for $\theta_Y \geq 90°$ [16, 17]. In the following, we will examine what determines the stability of the two wetting states in addition to θ_Y.

3. Impact of Texture on Superhydrophobicity

Not surprisingly, research has shown that the surface structure impacts the stability of the Wenzel and the Cassie state with respect to each other, as indicated by the Equations above. Several studies have therefore attempted to rigorously determine the structural parameters affecting the energy states of the system. In the literature, the investigation of these parameters is divided into two scenarios; one where the droplet is deposited on the textured surface, and one where the droplets condense on the textured surface. Although it is the latter case that interests us, it is instructive to initially understand the first, and simpler case.

3.1. Design Criteria for achieving Static Cassie Droplets

As there exists an infinite amount of possible surface geometries, the first challenge when developing a generic model for wetting states is to choose one that is fairly general, ordered, flexible and simple. One structure satisfying these criteria is the square array of square pillars with spacing b, width a, and height c. The structure is illustrated in Figure 6.

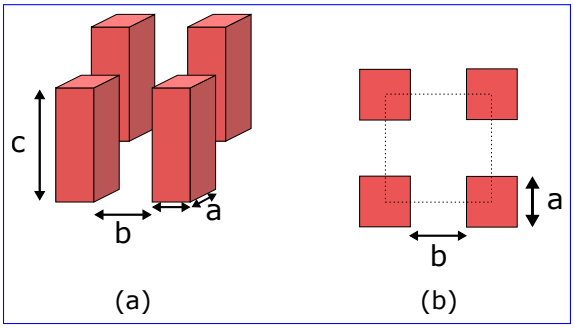

Figure 6: The geometry of the square pillar surface: (a) 3-dimensional view showing post width a, spacing b and height c; (b) top view of four nearest pillars, which outline a unit. Figures adapted from Sarkar et al.[18]

Using this structure, Sarkar et al.[19] developed a general expression for the free energy of a droplet as a function of the structure geometry, the apparent

contact angle and the penetration depth of the droplet into the structure. This expression was used in the later work by Sarkar et al.[18] to find the critical $\frac{b}{a}$-ratio, $(\frac{b}{a})_{crit}$, for a thermodynamically stable Cassie state:

$$\frac{b}{a} \leq \left(\frac{b}{a}\right)_{crit} = \sqrt{1 - \frac{4c\,cos\theta_Y}{a(1+cos\theta_Y)}} - 1 \tag{4}$$

Increasing a or c will decrease the minimum contact angle, i.e. loosen the restriction on the surface energy for achieving a stable Cassie state, see Figure 7. Increasing b will increase the same restriction. An increase in the pillar spacing to ~~diameter~~ width ratio, b/a, will also increase the minimum CA, see Figure 8. For achieving a droplet in the stable Cassie state, a large height, and small ratio between spacing and ~~diameter~~ width is favourable. As no nominally flat surface have been found that exhibit Young contact angle larger than 120°, Equation (4) also determines a maximum b/a along with a restriction for c. E.g. for $b/a \approx 3.1 \Rightarrow c > 4a$, depicted as a box in Figure 8.

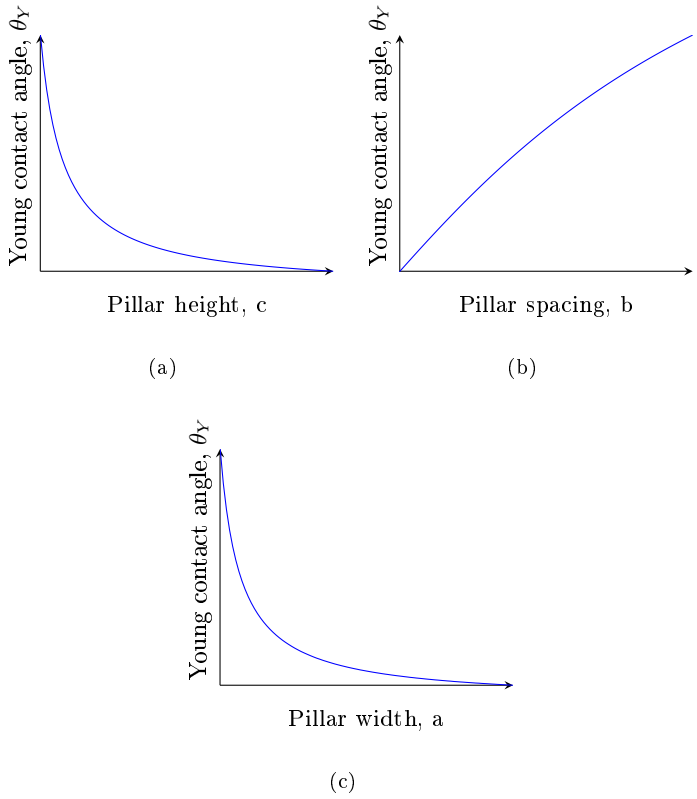

Figure 7: Minimum Young contact angle with respect to a) pillar height, b) pillar spacing, and c) pillar ~~diameter~~width, Equation (4). For increasing pillar height, c, and pillar ~~diameter~~width, a, (the other variables kept constant), the restriction on the contact angle decreases. For increasing only pillar spacing, b, the minimum contact angle increases.

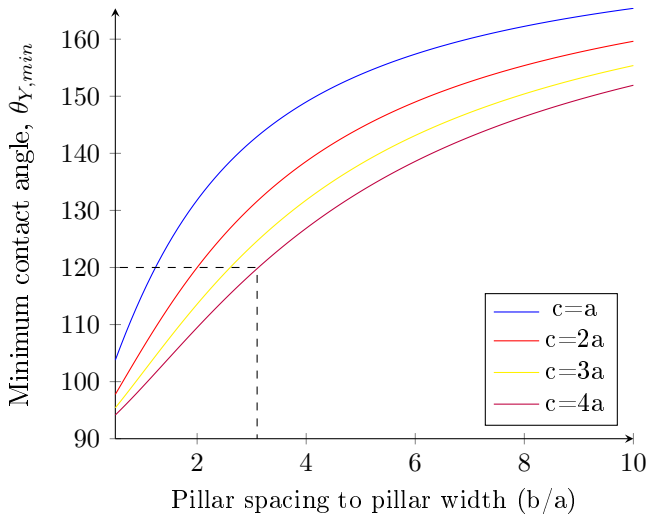

Figure 8: Minimum Young contact angle vs pillar spacing to pillar height (b/a).

Equation (4) corresponds exactly with the criteria for stable Cassie droplets developed by Zheng et al.[20]:

$$\eta = \frac{cL}{A} \qquad (= \frac{4c}{a} \text{in Sarkar's notation}) \tag{5}$$

$$\eta \geq \eta_{crit} = -\frac{1 - f_s}{f_s} \frac{(1 + cos\,\theta_Y)}{cos\,\theta_Y}, \tag{6}$$

where L and A are the pillar perimeter ($4a$) and cross-section area (a^2), respectively, and f_s is the fraction of wet apparent solid surface area from Equation (2). Although both models were derived from the expression of the Gibb's free energy, the procedures were slightly different. As a consequence, the two models are mutually verifying each other.

As established in the previous section, the Cassie state is not thermodynamically stable for $\theta_Y < 90°$. Moreover, it may not be stable even with $\theta_Y \geq 90°$. Sarkar et al. therefore developed an expression for the minimum Young contact angle for a stable Cassie state:

$$\theta_Y \geq \theta_{min} = sec^{-1}\left(\frac{4\frac{c}{a}}{1 - (1 + \frac{b}{a})^2} - 1\right) \tag{7}$$

Applying Equations (4) and (7) on the circular pillared structure[3] fabricated by Haimov et al.[23], yield $(\frac{b}{a})_{crit} \approx 3.7 \geq \frac{b}{a} = 2$ and $\theta_{min} \approx 99.6° \leq \theta_Y \approx 110°$. In other words, Sarkar et al. predict this structure to promote the Cassie state. The experimental results by Haimov et al. verify that the droplets indeed are in the Cassie state on this structure.

Equation (7) shows that the θ_{min} increases with increasing $\frac{b}{a}$. As a result, the requirement on the Young contact angle soon increases above the previously mentioned "limit" that has been observed experimentally on a flat surface: $\theta_Y \approx 120°$[4]. Nevertheless, the Cassie state has been observed on structures where the Wenzel state would have been the thermodynamically favoured state according to the previous design criteria [16, 24], suggesting that there must be a mechanism that kinetically stabilizes the Cassie state. The mechanism suggested by Sarkar et al. is the energy barrier set up by one of two metastable Cassie states, the sagging and the depinned Cassie states, shown in Figure 9. The metastable Cassie states act as energy barrier to the complete Cassie-to-Wenzel-transition.

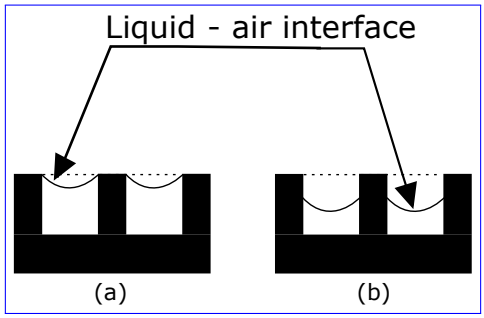

Figure 9: Illustration of the two metastable Cassie states found by Sarkar et al.[18]. The sagging state (a) and the depinned state (b).

[3]Circular pillars approximated as square for the occation. c=10μm, a=1μm and b=2μm. $\theta_{Y\ dodecanethiol/Au} \approx \frac{\theta_{adv}+\theta_{rec}}{2} = \frac{112°+107°}{2} \approx 110°$[21, 22]

[4]Though some claim that secondary nanostructures count as small enough to be part of the intrinsic (flat) surface, and thus enabling $\theta_Y > 120°$[17, 18]

The energy barrier induced by these metastable Cassie states have been found to depend on the structure geometry as well as the surface chemistry (in terms of θ_Y). Not surprisingly, the requirements on the relevant parameters are less strict than for the thermodynamically stable Cassie state. The requirements are summarized in Table 1.

Table 1: Design criteria for droplets in stable and metastable Cassie states [18]

State	**Geometric requirements**	**Material requirements**
Stable Cassie	$\frac{b}{a} \leq (\frac{b}{a})_{crit} = \sqrt{1 - \frac{4c\ cos\theta_Y}{a(1+cos\theta_Y)}} - 1$	$\theta_Y \geq \theta_{min} = sec^{-1}\left(\frac{4\frac{c}{a}}{1-(1+\frac{b}{a})^2} - 1\right)$
Sagging Cassie	$0.75 < \frac{c}{a} < 0.9$ & $(\frac{b}{a})_{crit} < \frac{b}{a} < (\frac{b}{a})_{sag} = \frac{1+cos\theta_Y}{\sqrt{(2\frac{c}{a})^2-2(1+cos\theta_Y)}}$	$90° < \theta_Y < 105°$
Depinned Cassie	$(\frac{b}{a})_{crit} < \frac{b}{a} < (\frac{b}{a})_{pin} = \frac{(1+cos\ \theta_Y)}{\sqrt{(2\frac{c}{a})^2-2(1+cos\ \theta_Y)}}$	NA

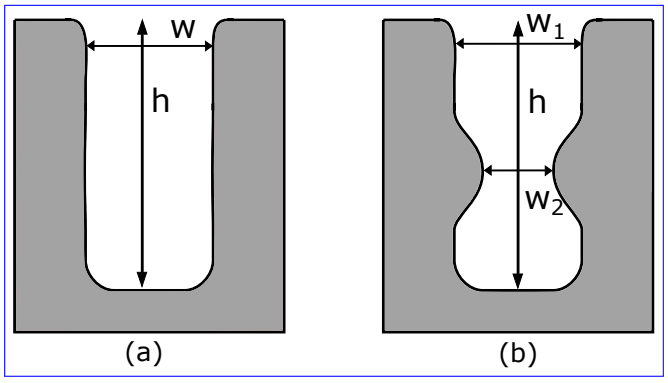

Figure 10: The square pillar geometries without (a) and with (b) scallops, used by Hensel et al. (2014)[25]

In the above mentioned studies, the surface geometry is utilized to promote a stable or a stabilized Cassie state. Hensel et al.[25] investigated the energy barriers induced by sidewall features of the pillars in a square pillared structure (see Figure 10) further. Using $\frac{b}{a}$-ratios supporting the Cassie state at atmospheric pressure, they found a clear relation between the width, w, of the cavities and the breakthrough hydrostatic pressure. As the width increases, the breakthrough hydrostatic pressure decreases for the structure with smooth sidewalls. Moreover, there is an increase in the breakthrough pressure for the Cassie-to-Wenzel-transition for sidewalls with scallops, (b) in Figure 10, compared with smooth sidewalls, (a) in Figure 10, at equal top cavity width. The increase is caused by the change in width, from w_1 to w_2 in Figure 10 (b), and sidewall angle as the solid-liquid contact line slides down the side wall. These experimental results match well with the analytical model that was developed.

3.2. Design Criteria for Condensing Cassie Droplets

We now have a clear idea of how feature spacing, width and morphology impact the droplet state of a static droplet. It is of course tempting to assume that the same parameters affect the droplet state of condensing droplets. During condensation, however, the droplets may not only nucleate on the top of the surface structure, but also inside the structure. One important property in this sense is the nucleation radius of the specific vapor, a measure of the initial drop nuclei radius. If the nucleation radius is smaller than the feature spacing, nucleation may occur within the features.

Recall from the previous section that for many structures the Cassie state is kinetically stabilized by an energy barrier preventing the Cassie-to-Wenzel-transition. In the case of nucleation inside the structure, the challenge is reversed. Here the structure must *promote* a Wenzel-to-Cassie-transition. Although this latter case may add to the challenges associated with stabilizing a Cassie state, it is actually the desired case from a heat exchange point of view. This is because the emerging droplets explore more of the surface area during nucleation and growth in the Wenzel state, and thus increases the heat

exchange, followed by easy removal after Wenzel-to-Cassie transition[26].

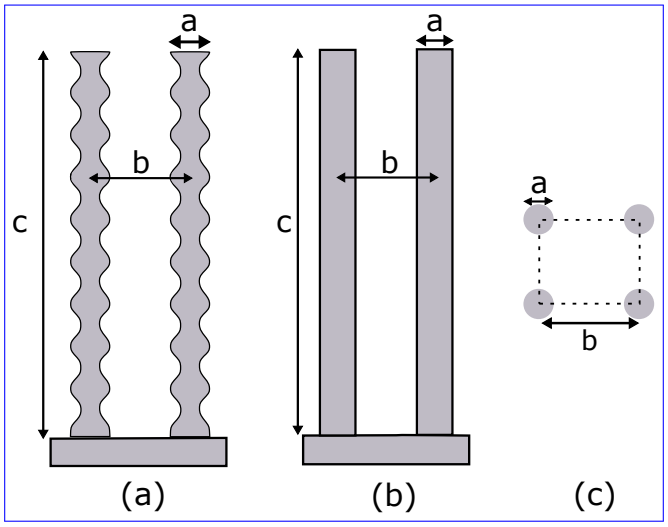

Figure 11: Circular pillar geometries fabricated by Enright et al.[26]: (a) Si nanopillars; (b) Si micropillars; (c) Top view of four nearest pillars, which outline a unit

To investigate the difference between deposited Cassie droplets and Cassie droplets condensing on a surface, we go back to our structure comprising the square array of square pillars from Figure 6. Enright et al. [26] investigated the water vapor condensation on this structure[5] with different spacings and sidewall features (see Figure 11). Condensation on two different structures similar to that shown in Figure 11(a) with diameter $a = 300\,\text{nm}$, height $c = 6.1\,\mu\text{m}$ and spacings $b_1 = 2\,\mu\text{m}$ and $b_2 = 4\,\mu\text{m}$ were investigated. Using Equations (4) and (7) [6], we find that:

$$\theta_{min\,b_1} \approx 114^\circ \leq \theta_Y \approx \theta_{adv} = 121.1^\circ \;\&\; \frac{b}{a} = 6.7 \leq \left(\frac{b}{a}\right)_{crit} \approx 8.4 \qquad (8)$$

[5] They used circular pillars, which again are approximated as square to fit Sarkar et al.'s models

[6] Where we use θ_{adv} ~~in stead~~ instead of θ_Y since condensing droplets are continually growing

$$\theta_{min\,b_2} \approx 135.7^\circ \geq \theta_Y \approx \theta_{adv} = 121.1^\circ \;\&\; \frac{b}{a} \approx 13.3 \geq \left(\frac{b}{a}\right)_{crit} \approx 8.4 \qquad (9)$$

According to Equation (8) the surface with spacing b_1 should promote droplets in the stable Cassie state. As shown in Figure 12(a), the surface with spacing b_1 does indeed promote droplets in the Cassie state.

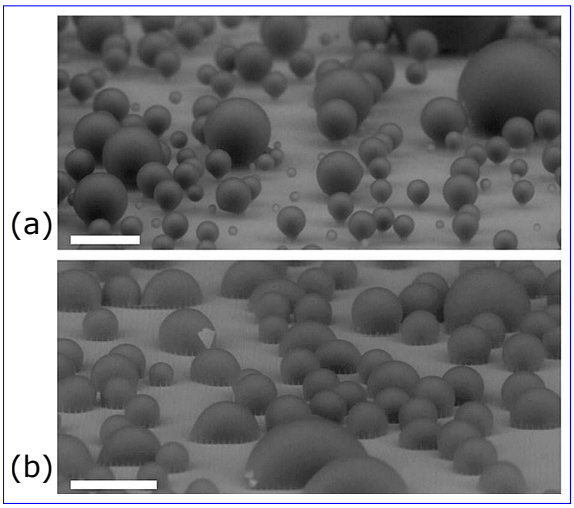

Figure 12: Condensation on surfaces similar to structure in left pane of Figure 11 with spacing (a) b_1=2 µm and (b) b_2=4 µm. Surfaces exhibit formation of Cassie droplets and Wenzel droplets, respectively. Scale bars = 60 μm. Reprinted with permission from Enrigth et al. [26]. Copyright 2012 American Chemical Society.

For the surface with b_2-spacing, the calculations in Equation (9) indicate that the Wenzel state is thermodynamically more stable than the Cassie state. In agreement with this, Figure 12(b) shows droplets in the Wenzel state. Hence, Sarkar et al.'s mathematical predictions for the stability of static droplets are in agreement with experimental results also for condensing droplets. On the other hand, the criterion for a metastable depinned Cassie droplet given in Table 1 is also fulfilled:

$$(\frac{b}{a})_{crit} \leq \frac{b}{a} \leq (\frac{b}{a})_{pin} \approx 64 \qquad (10)$$

Nevertheless, it is sensible that this surface supports Wenzel droplets. Due to

the large spacing compared to critical nucleation radius, typically a few nm [27], nucleation occurs all over and within the structure. Droplets nucleating and growing inside the structure have already overcome the energy barrier that the depinned state poses. Thus the droplets remain in the Wenzel state.

Moreover, Enright et al. investigated the relation between the $\frac{c}{a}$-ratio of smooth-walled pillars with constant diameter and pitch, and the stability of the condensing Cassie droplets. They found that the depinning of contact lines stabilizing the metastable Cassie state depends on pillar height, where the stability increases with the height. Their results are therefore in agreement with Equations (4) and (7), which predict less strict requirements on the θ_Y and $\frac{b}{a}$-ratio for a stable Cassie state as the $\frac{c}{a}$-ratio increases.

Nosonovsky et al.[28] also investigated the square array of cylindrical pillars with diameter $a = 5\,\mu\text{m}$, height $c = 10\,\mu\text{m}$ (series 1), and $a = 10\,\mu\text{m}$ and $c = 14\,\mu\text{m}$ (series 2). Both series included surfaces with a range of pitches, p ($= a + b$ in Sarkar et al.'s notation). It was found experimentally that the critical $\frac{a}{p}$-ratio for a Wenzel-to-Cassie transition is $(\frac{a}{p})_{crit} = 0.51$. Only the three smallest pitches in each series exhibit $\frac{a}{p} \geq 0.51$. This is in agreement with Sarkar et al.'s criteria for droplets in the stable Cassie state (Equations (4) and (7)), which is fulfilled by the three smallest pitches in each series.

So far we have only regarded the structural geometry and chemical properties of the surfaces. However, the mechanical properties of the material may also promote or inhibit the Cassie state. Pillars fabricated of soft materials may bend as the droplets grow between the pillars. As a result the energy of the entire system increases, and flooding of the structure may become energetically favourable [29]. Consequently, the choice of material is important with regard to the intrinsic Young contact angle, but also the mechanical properties of the material. Copper and copper oxides are therefore frequently used due to their mechanical durability. Zhu et al. [30] is one of the groups that successfully fabricated clustered copper nano-needles that were able to promote a Wenzel-to-Cassie-transition. Consequently, droplets were allowed to nucleate at the base, exploring the surface area and increasing the heat transfer rate, meanwhile a

continuous shedding of macrodroplets was maintained.

Although the results from the condensation experiments are not in complete agreement with the design criteria from the static droplet experiments, the trends are similar. Hence, the design criteria from static droplet studies may work as a good starting point for fabrication of surfaces for condensing droplets.

3.3. Design of Superhydrophobic Surfaces for Water Condensation

As mentioned earlier, there is a wide range of surface structures that may promote droplets in the Cassie state. Recent research has shown that surfaces combining different structures and/or chemistries can yield high degrees of superhydrophobicity. In the following, we will therefore discuss some of these surfaces.

3.3.1. Micro- and Nanostructured Surfaces

Micro- and nanostructured surfaces, often named hierarchical structures in the literature, are surfaces with a combination of microstructure and a secondary nanostructure (applied on top of the microstructure as illustrated in Figure 13).

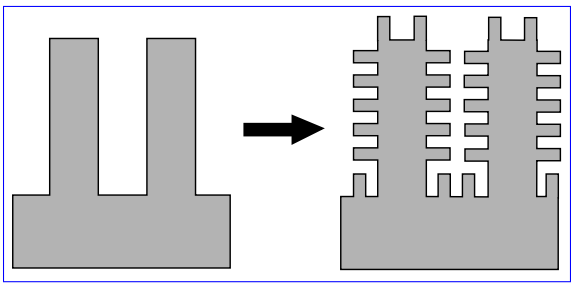

Figure 13: Illustration of microstructure and hierarchical micro- and nanostructure.

Several groups have successfully fabricated such surfaces with a variety of materials and morphologies. CuO/Cu surfaces such as the one fabricated by He et al. [31] are promising. These surfaces have microsized holes in a square pattern inside which nanosized randomly oriented nanoneedles are grown. The inclusion of the nanoneedles raise the contact angle to above 150°, which means that superhydrophobicity is achieved.

For a systematic approach of investigating the role ~~of hierarchicality~~structures on different length scales, it is suitable to look at the study by Lo et al. [16]. They investigated the water vapor condensation on micro- and nanostructured surfaces compared to plain microstructured surfaces. Two types of microstructures were used: parallel microgrooves (PMG) and cross-sectioned microgrooves (CMG). Inside the microgrooves, silicon nanowires (SiNW) where randomly and densely grown, which constitute the nanostructure of the surface. Although highly pinned Wenzel droplets are observed on the plain CMG[7] and PMG surfaces, the hierarchical surfaces (CMG/SiNW and PMG/SiNW) both exhibit continuous shedding of droplets. This indicates that the secondary structure promotes Cassie droplets with low CAH. Interestingly though, the PMG/SiNWs exhibit a magnitude smaller cycle time (i.e. the time from nucleation to departure of a droplet) compared to CMG/SiNW. Thus, the pinning of droplets must be larger on the CMG/SiNW than the PMG/SiNW. A small cycle time is desired because it indicates a large heat and mass transfer rate [27]. On the other hand, the SiNW on a smooth surface also exhibits smaller cycle time than CMG/SiNW. Consequently, the micro- and nanostructured surface might not always yield better results.

According to classical nucleation theory (CNT), the nucleation rate on a microstructured surface (surface with microsized features) is higher than that on a nanostructured surface. The Gibbs free energy of formation of droplets is given by

$$\Delta G = \frac{4}{3}\pi r_e^2 \sigma_{lv} F - 4\pi\sigma_{lv} F (r_c - r_e)^2 \tag{11}$$

where r_e is the equilibrium droplet radius, σ_{lv} the liquid-vapor surface tension, $F = 0.25(2 - 3\cos(\theta) + \cos^3(\theta))$, θ is the equilibrium contact angle, and r_c is the roughness diameter.

As seen in Figure 14 a microsized roughness (cavity dimension) will increase

[7] Note that the observations correspond to the predictions in Equations (4) and (7) while Nosonovsky et al.'s limit fail for the relevant dimensions

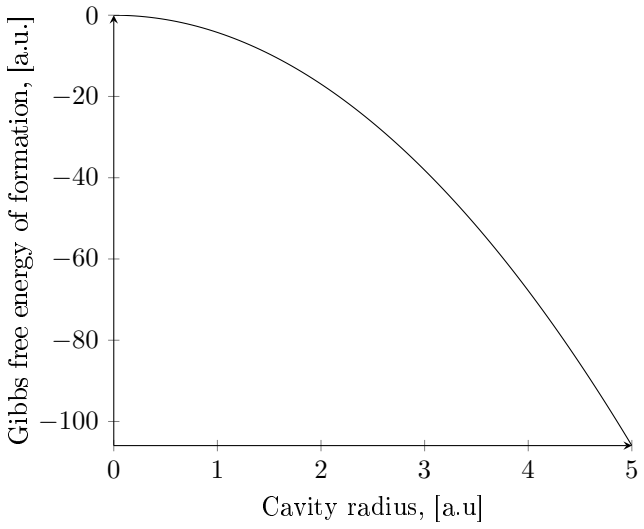

Figure 14: Gibbs free energy of nucleation with increasing cavity dimension (Equation (11)). The higher the dimension, the easier the formation of nuclei.

the nucleation rate by lowering the barrier towards nucleation. In the work by Lo et al. [27] it is found that more nucleation and condensation occurs on the CMG and PMG surfaces, compared to SiNW surfaces, which supports the theoretical results.

3.3.2. Surface with Hydrophilic and -phobic Domains

One of the main challenges in a dropwise condensation heat exchanger is how to achieve high nucleation rates while maintaining sustainable shedding of droplets. The two processes are determined by different and opposing mechanisms. While hydrophobic surfaces promote sustainable droplet departure, they also reduce the nucleation density. There have therefore been several attempts to develop a type of hierarchical surface structure with hydrophilic and hydrophobic domains[32, 33].

Chen et al. [33] designed silicon surfaces with pyramidal structures covered by nanograss everywhere except for the lower base of the sides of the pyramids. Thus, surfaces with global superhydrophobicity, but local hydrophilicity

were obtained. These surfaces were reported to exhibit sustainable dropwise condensation behaviour with enhanced droplet nucleation and droplet departure volume. In fact, the surface with the smallest spacing between the pyramids (S=20 µm) showed a 450% increase in drop self-removal volume and a 65% increase in drop number density compared to the flat surface covered with nanograss. The massive increase in droplet self-removal volume is attributed to the coalescence driven out-of-plane jumping.

The coalescence driven out-of-plane-jumping is believed to be caused by release of excess surface energy as two or more droplets coalesce. The released energy propel the resulting droplet from the surface. While this behaviour is observed on multiple surfaces with extremely low surface adhesion [34, 35, 30], the mechanism of this self-removal is not fully understood. Enright et al. [36] investigated the phenomenon further. Their study showed that this kind of self-removal is fundamentally inefficient; less than 6% of the released surface energy at coalescence was transferred to translational energy removing the droplet from the surface. As a consequence, this kind of self-removal is unlikely to occur for immobile or semi-mobile Wenzel droplets (as the adhesion energy between the droplet and the surface is larger). Thus, the importance of promoting the formation of Cassie droplets for heat exchange applications is reinforced.

On the other hand, the results from Boreyko et al.[9] indicate that the energy released during coalescence is higher than the Wenzel-to-Cassie-transition energy barrier. Thus the coalescence may improve the droplet mobility, even in cases where the resulting translational energy is not sufficient for complete self-removal. Moreover, the yield of the self-removal may be increased by preventing droplets from returning due to gravitational drag (for vertical surfaces) or entrainment in the vapor flow (either adjacent to the surface or towards the surface, depending on the conditions of the condensation). For example, Miljkovic et al. enhanced the yield through the use of an external electric field that prevented droplet return [37].

3.4. Coating with a low surface energy chemical

In any case of surface structuring, either on one or more length scales, it is often necessary to additionally coat the surface with a thin film of a low surface energy compound to achieve superhydrophobicity [38, 39]. Common low surface energy materials are polymers with surface functional groups, such as -CF_2, -CF_2H and CF_3. The fluorinated or perfluorinated materials do not influence the roughness of the surfaces, but can largely influence the surface energy and therefore the contact angle of the liquid.

3.4.1. Superhydrophobicity by Liquid-Infusion

So far in this paper, only surfaces with micro- and/or nanostructures have been discussed. The superhydrophobicity of these surfaces depends on the surfaces' ability to stabilize the droplets in the Cassie state. Although many of these surfaces exhibit superhydrophobicity, they may not be suitable for industrial use. In industrial applications, the surfaces will be subjected to varying conditions and various contaminants that may destabilize the Cassie state [35]. In addition, many of the surfaces are vulnerable to mechanical abrasion due to the fragile nature of the surface structures. Hence, the wetting properties may be greatly affected[11, 40]. One promising solution is to use slippery liquid- or lubricant-infused porous surfaces (SLIPS) ~~in stead~~instead. The main idea is schematically shown in Figure 15.

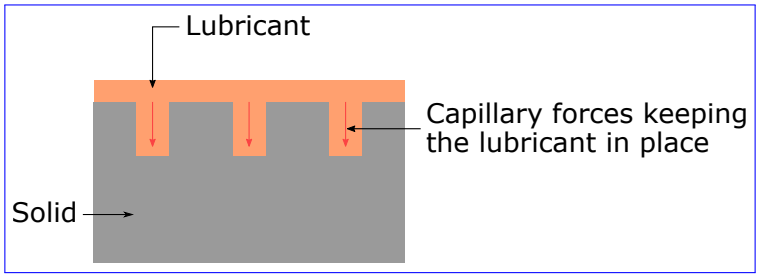

Figure 15: A SLIPS shown schematically

The capillary forces created by the micro- or nanostructure of the underlying solid are utilized to contain a viscous lubricant within the structure. Since an

excess of lubricant is applied on the solid surface, a semi-mobile, smooth top layer is created. Thus, it is the properties of the lubricant that mainly determines the wetting properties of the entire system. As opposed to a normal flat solid surface, the surface of a SLIPS can be molecularly smooth, resulting in a small friction, and hence, small CAH. The surface will therefore be "slippery" even when the surface tension of the lubricant is not small enough to attain superhydrophobicity. In addition, the semi-mobile layer introduces an additional robustness, as discussed later in this section.

Although the underlying surface of the SLIPS is less important for the surface wetting properties, it is essential for the sustained containment of the lubricant within the surface structure [40]. The surface structure induced capillary forces are, as mentioned, important in this sense. In addition, the solid surface chemistry must be compatible with the lubricant, and reinforce the strong attraction between the underlying solid surface and the lubricant. If the attractive forces are too weak, water droplets condensing (or deposited) on the surface may displace the lubricant. Hence, the surface may loose its slippery properties [11]. Also, to further decrease probability of liquid displacement of the lubricant, the lubricant and the liquid must be immiscible.

In the scenario of low attractive capillary forces, the impact of the underlying surface chemistry was demonstrated by Kajiya et al. [41]. They showed that the water droplets may displace the lubricant during condensation and growth. Nevertheless, the surface can retain its hydrophobic state if the underlying surface is water repellent. At further growth, the droplets may detach from the underlying surface.

The increased robustness of the SLIPS arises, as mentioned, from the semi-mobile layer. While the wetting properties of a textured superhydrophobic surface are compromised beyond repair upon contamination or mechanical abrasion, the mobility of the lubricant of a SLIPS causes the surface to be self-healing[40, 42]. In addition, combinations of micro- and nanostructures can be utilized to create superhydrophobic SLIPSs that are insensitive to the wetting state of the droplet (i.e. whether it is in the Wenzel or the Cassie state). This

was demonstrated in the study by Dai et al. [43]. In Figure 16 a schematic drawing of Dai et al.'s surfaces exhibiting (a) slippery Wenzel state (sliding angle = 18°) and, (b) slippery Cassie state (sliding angle = 8°) is shown. The slippery Cassie state is caused by the superhydrophobicity of the surface, while the slippery Wenzel state occurs due to the slipperiness of the lubricant. Consequently, the surface exhibited a low CAH and high droplet departure rate even if the Cassie droplet for some reason collapsed. Thus, they created a surface that will be less vulnerable to different conditions and contaminations.

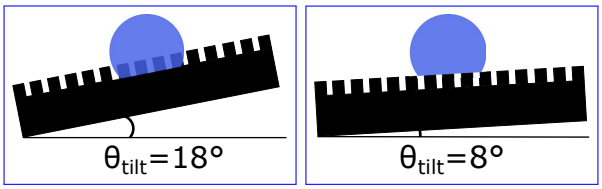

(a) (b)

Figure 16: Schematic of the droplets in different states on Dai et al.'s s SLIPS[43]. a) Droplet in the slippery Wenzel state, b) droplet in the slippery Cassie state.

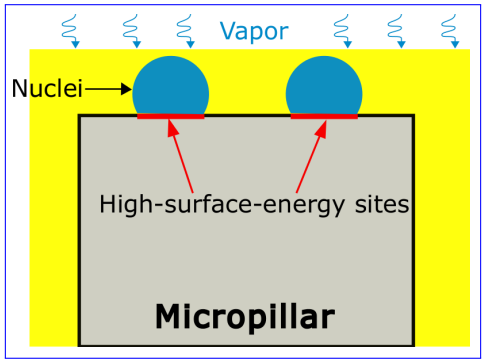

Figure 17: SLIPS utilizing hydrophilic and -phobic domains on underlying surface for controlled nucleation. Figure adapted from Xiao et al. (2013)[44]

Hierarchical structures may also be utilized in SLIPSs to promote dropwise water vapor condensation. Xiao et al. [44] investigated the water condensation on a SLIPS with hydrophilic domains in the underlying surface (see Figure 17).

They observed that the lubricant layer covering the underlying pillars was thin enough for the water vapor to penetrate. Thus the vapor nucleated on the hydrophilic domains. During growth, the droplets detached from the underlying surface and attained a hydrophobic state[8]. Increased nucleation density and decreased droplet departure diameter compared to the same surface without infused lubricant was shown.

Several mechanisms can cause the failure of superhydrophobicity or the transition to filmwise condensation on SLIPS [45]. Lubricant displacement is already mentioned, which can be caused by low capillary forces between lubricant and solid, or that spreading coefficient of the lubricant on the condensate in the presence of gaseous condensate is positive [46]. Miscibility of the condensate and the lubricant will cause them to mix and depletion of lubricant will gradually occur as the droplets are removed from the surface. Another failure mechanism is cloaking, for which spreading of the lubricant on the condensate is the preferred state and a thin film of lubricant will spread on the condensate droplet [47]. The removal of droplets, e.g. by gravity, will then cause removal of lubricant and with time the lubricant is consumed. Even if cloaking is avoided, there is a chance that the lubricant will not spread on the structure in the presence of the condensate and either spread only directly underneath the droplets or everywhere except underneath the droplets, causing a Wenzel state.

3.5. Challenges and future outlook

To complicate things, experimental conditions such as temperature, presence of non-condensable gases and gas flow may affect the condensation of water vapor. In addition, the mechanical and thermal properties of the solid substrates are important to consider when transferring the technology to the industry.

Most of the studies discussed in this work are performed under ideal conditions for environmental Scanning Electron Micsroscope. That is, low temper-

[8] Xiao et al. claim superhydrophobicity, but although contact angle hysteresis was 3°, contact angle was only 110°

ature, semi-vacuum and "static" conditions. This is far from industrial conditions, where higher operating temperatures, gas flow and saturated water vapor (as opposed to air or semi-vacuum) conditions are required. These conditions might introduce additional challenges to promote and maintain dropwise condensation. Increased temperatures reduce the surface energy of the water droplets and therefore, make it challenging to obtain the Cassie state [38]. The literature is, however, not conclusive on whether water vapor conditions will affect the wetting state significantly. Weisensee et al. [6] observed a finite reduction of contact angles on flat surfaces of Teflon while the remainder of the tested textured surfaces maintained their wetting states in saturated water vapor conditions, compared to water condensation in an air environment.

Torresin et al. [38] investigated water vapor condensation and heat transfer under vapor flow conditions at high operating temperatures (110 °C). The high temperature caused formation of Wenzel droplets despite the fact that the surface promoted Cassie droplet formation at lower temperatures. All the same, they observed increasing heat transfer with increasing gas flow. The gas flow created a shear force that moved the initially immobile Wenzel droplets, and thus increased the heat transfer by decreasing the droplet departure radius. On the other hand, the gas flow also introduced higher wear on the surface and over time the degradation was significant. In fact, Torresin et al. found that the condensation on their superhydrophobic nanotextured surfaces went through a transition from dropwise to filmwise condensation after five days of testing. This was caused by the degradation of the nanostructures and the deterioration of the hydrophobic monolayer from the shear stress generated by the vapor flow. After the transition the surfaces performed worse than "normal" surfaces for filmwise condensation with respect to the heat transfer. Degradation, of any kind or reason, is therefore found to be detrimental to the performance of superhydrophobic surfaces, and is still a huge unresolved issue, and therefore, poses great challenges for industrial applications.

In most of the studies discussed in preceding sections, heat transfer rates have not been measured. Instead, it is assumed and predicted by models, e.g. [48],

that the heat transfer increases for dropwise condensation compared to filmwise, and also for Cassie droplet formation rather than Wenzel. On the other hand, the trapped vapor underneath the liquid droplets in the Cassie state may create additional heat transfer resistance [38], reducing the condensation rate, and it is therefore necessary to minimize this vapor volume while on the same time ensuring droplet mobility. Therefore, there are indications that the quasi-Cassie state (a metastable mix of Wenzel and Cassie) yields the highest heat transfer [49]. Aiming for surfaces promoting the pure Cassie state could therefore be a mistake.

Another solution could be not to aim for superhydrophobicity at all. Studies have shown that a slightly hydrophilic surface could promote dropwise condensation [50, 51]. In addition, high mobility of the droplets can be induces by introducing superhydrohilic trenches ($\theta \approx 0$) on the surface. The trenches can lead the droplets away from the surface and a surface for efficient nucleation, growth and drainage is possible. The heat transfer coefficient for such a surface is measured to be up to 34.4 % higher than for a purely hydrophilic surface [51].

4. From Syperhydrophobicity to Superlyophobicity

While surfaces used for water vapor condensation have been subjected to extensive research, literature on surfaces for dropwise CO_2 condensation is virtually non-existing. There is, however, an increasing amount of studies on superlyophobic surfaces[9]. These are surfaces that per definition exhibit $\theta^* \geq 150°$ and $\Delta\theta \leq 10°$ for any liquid. Experimentally, it is of course immensely time consuming to test the wetting properties of a surface for all possible liquids. The focus have therefore been on liquids with low surface tension, mostly organic compounds, such as ethanol, hexane and hexadecane. To understand the potential changes in surface chemistry and structure design criteria as water is

[9] A conglomeration of different terms appear in this field; superoleophobicity, superamphiphobicity etc., rigorous definitions of these terms can be found in the introduction, Section 1

replaced by CO_2, we therefore look into the similar changes as we move from superhydrophobic to superlyophobic surfaces.

Although it is tempting to assume that the surface requirements for Cassie droplet stabilization are equal for superlyophobic and -hydrophobic surfaces, dramatic reductions in liquid surface tension cause the conditions for droplet formation to change considerably. Recall from Section 2.2 that the Cassie state is always thermodynamically more unstable than the Wenzel state for $\theta_Y < 90°$. As long as water is the condensate, there is a range of materials exhibiting $\theta_Y \geq 90°$. Thus, with the "right" surface structure, formation of stable Cassie droplets is attainable. However, for the low surface tension condensates, the range of materials diminishes. Formation of thermodynamically stable Cassie droplets may therefore be impossible. On the other hand, from Section 3.1 we know that the surface structure can introduce energy barriers preventing Cassie-to-Wenzel transition. Even though the design criteria described in this section was developed for $\theta_Y \geq 90°$, it may be possible to introduce similar energy barriers for $\theta_Y < 90°$. In that way, metastable Cassie droplets may be attainable.

4.1. Impact of Texture on Static Cassie Droplet Formation

As with superhydrophobic surfaces, attempts have been made to rigorously characterize the impacts of various surface features on the wetting properties of superlyophobic surfaces [52, 53].

Tuteja et al. [52] investigated the advancing and receding contact angles of liquids with a range of surface tensions on electrospun surfaces of blends of (hydrophilic) PMMA and[10] (hydrophobic) fluorodecyl POSS[11], a polyhedral crystalline solid material. Even at low weight percent of fluorodecyl POSS (<2wt%), high apparent advancing contact angles, $\theta^*_{adv} > 90°$, with both water and low surface tension liquids were observed. Since the surfaces are hydrophilic

[10] Poly(methyl methacrylate)

[11] fluorodecyl polyhedral oligomeric silsesquioxane

at these wt%, indicated by $\theta_Y < 90°$ on the smooth corresponding surface, we would expect $\theta^*_{adv} < \theta_{adv} < 90°$ according to Equation (1). The droplet must therefore be in a metastable Cassie state that obstruct the transition to the Wenzel state. This hypothesis was confirmed by releasing the droplets onto the surfaces from a height, where the impact energy caused a Cassie-to-Wenzel-transition and decreased θ^*_{adv}. The metastable Cassie state was observed for a range of liquid alkanes even though all the surfaces were oleophilic (wettable for oily substances). The CAH for the low surface tension liquids were, however, large, especially for low wt% of fluorodecyl POSS.

4.1.1. Design Criteria

Wu et al. [53] investigated the impact of the surface texture on the introduced energy barrier for Cassie-to-Wenzel-transition further. They formulated design criteria for sustained superlyophobicity. Based on those design criteria, they showed that the T-shaped structure satisfying the following inequalities (Equation (12)), was the most mechanically robust geometry[12].

$$\begin{aligned} R &\geq \frac{(\frac{1}{f_s} - 1)D}{n\, sin\theta_Y} \\ H &\geq \frac{L}{2} tan\frac{\theta_Y}{2} \end{aligned} \tag{12}$$

where R is the macroscopic radius of the droplet, H and D are height and diameter of the T-shape, respectively (see Figure 18(a)), L is the distance between two adjacent caps and f_s is the solid fraction from Equation (2). Schematic diagrams of the individual micropillars and the chemistry of the T-shaped surface are shown in Figure 18(b).

[12]NB. This model is derived for droplets deposited on the surface

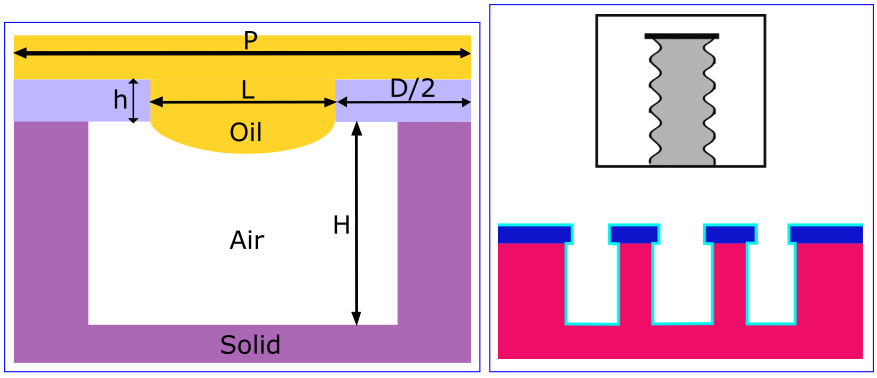

(a) (b)

Figure 18: (a) Illustration of the geometry of the T-shape. Figure constructed after model by Wu et al. [53]. (b) Chemistry of the T-shape shown schematically (upper). The colours describe different materials, with turquoise being 1H, 1H, 2H, 2H-perfluoro-octyltrichlorosilane (PFOTS), red Si and blue SiO_2. Sidewall features of this T-shaped surface (lower). Figures adapted from Wu et al. [53]

Several geometries meeting the design criteria by Wu et al. were tested for lyophobicity with water and hexadecane. Apparent contact angles, θ^*, as high as 170° for water and 167° for hexadecane were obtained for the surface shown in Figure 18(a). The contact angle hysteresis, $\Delta\theta$, on this surface was approximately 8° for both liquids, which confirms the superlyophobicity of the surface. Interestingly, the water and hexadecane θ^* and $\Delta\theta$ were almost the same for all the tested geometries (also those with $\theta^* < 150°$), but greatly varying with solid fraction, f_s (see Equations (1) and (2)). This indicates that f_s dominates the wetting properties of the surface when the droplet is in the Cassie state. The role of increasing f_s for a hexadecane droplet ($\theta_Y = 50°$) on Si is shown in Figure 5. The solid fraction on the surfaces in Figure 18(a) is 0.08 [53], which according to Equation (2) results a contact angle of 169°. This is in good agreement with the experimental results of 170° (water) and 167° (hexadecane).

Wu et al. [53] also tested the values of $\Delta\theta$ against three existing models;

the Wenzel and Cassie equations (Equation (1) and (2)) for advancing and receding contact angles, the linear average model by Extrand [54], and the local differential parameter model by Choi et al. [55]. While the advancing contact angles are in decent agreement with the two latter models, the receding contact angles are not predicted satisfactory for all cases with any of the models. One explanation is that the static contact angle, θ_Y, is assumed to be the same on a flat and a rough surface. However, the static contact angle may vary according to the degree of pinning on the asperities of the structures, and the predictions of contact angles are therefore not exact.

4.1.2. Micro- and Nanostructured Surfaces

As with water condensation, hierarchical structures featuring micro- and nanostructures have been observed to yield superlyophobicity [56]. Mazumder et al. [14] fabricated a superomniphobic ~~(water and oil repellent)~~ surface of nanopillars (glass/SiO_2) with branching structures on top (SiO_2). Contact angles of 172°, 163° and 153° with water, oleic acid and hexadecane, respectively, were obtained. The contact angle hysteresis for the respective liquids were $< 3°$, $< 4°$ and $< 6°$. However, this structure is fragile and susceptible to mechanical abrasion. To improve the robustness of the surface, nanonodules were deposited instead of the branching structure. While the resistance to mechanical abrasion improved, the contact angles decreased, and became only slightly higher than those on the primary nanopillars.

Recall the criteria developed by Sarkar et al. [18]. Not surprisingly, we find that the geometry of the nanopillared structure (without a secondary structure on top) does not satisfy the criteria for formation of hexadecane droplets in the stable Cassie state. Moreover, the critical value for the spacing to width ratio, $\left(\frac{b}{a}\right)_{crit}$, assumes a negative value. According to Sarkar et al.'s criteria (see Table 1), the metastable states for this geometry are automatically excluded too. However, experiments show that the contact angle is $\theta^* = 104 > \theta_Y$. On the other hand, the criteria for metastable (sagging) Cassie droplets are partially satisfied since $\frac{b}{a} \leq \left(\frac{b}{a}\right)_{sag}$. Although this single example surface of Mazumder

et al. is not sufficient to conclude, it can be used as an indication of that the design criteria developed by Sarkar et al. are applicable to superlyophobic surfaces too. In any case, they can constitute a starting point for the design of a superlyophobic surface.

4.1.3. Lowering the surface energy

As stated previously, a reduction in surface energy by coating with a low energy material such as fluorines may be necessary for superhydrophobicity. To achieve superlyophobicity, on the other hand, literature shows that this step may be crucial [57]. A variety of low surface energy materials are used in the literature, but a common feature is the small or large degree of fluorination of an organic compound. Examples are 1H,1H,2H,2H-heptadecafluorodecyl [58] and 1H,1H,2H,2H-perfluoro-octyltricholorosilane [53, 11].

4.2. Formation of Condensing Cassie Droplets

As we move from liquid droplets deposited on the surface to condensation of the liquid, we face the same challenges as discussed for superhydrophobic surfaces. The major question is: Will the droplets nucleating at the base of the surface structures transition to a Cassie state? This is, if possible, an even greater challenge for superlyophobic surfaces compared to superhydrophobic surfaces because we have $\theta_Y < 90°$. Thus, the Wenzel state is always thermodynamically favourable. In addition, it is probable that the energy barrier for a Wenzel-to-Cassie-transition becomes even greater. Consequently, the requirements on the surfaces become even stricter.

A few attempts have been made to create superlyophobic surfaces for condensation. Rykaczewski et al. [11] tested the wetting properties during condensation of several structures including Al-SiO_2 nanotextured, polymer solution re-entrant (or overhanging) superomniphobic, Si micropost textured surfaces, and lubricant infused surfaces (SLIPS). Condensation was also tested on all the surfaces impregnated with a lubricant. The results from these experiments were mixed. In fact, the overall performance of a fluorosilane-functionalized, smooth

surface[13] was best. The impregnated surfaces were generally more likely to induce dropwise condensation than the nanotextured and superomniphobic surfaces, which both showed filmwise condensation for all or nearly all liquids.

The formation of films on the nanotextured and superomniphobic surfaces indicates that the condensates nucleate within the structure. Moreover, the structures are unable to surpass the energy barrier for a Wenzel-to-Cassie-transition. As a consequence, the liquid floods the structure. Decreasing the dimensions of the surface structure below the critical radius of nucleation may prevent nucleation within the structure. This comes, however, at the cost of increased fabrication cost and complexity.

Although the SLIPSs appear to perform better than the textured superlyophobic surfaces for dropwise condensation of liquids with low surface tension, several challenges stil remain. Some of these are illustrated in the above described study by Rykaczewski et al.. The condensing liquid displaced the lubricant on several occasions, and caused filmwise rather than dropwise condensation. In addition, on some of the rougher underlying structures, the lubricant layer was not thick enough to cover the structure, and instead filmwise condensation was promoted. In other words, the lubricant must exhibit good adhesion to the solid surface, while maintaining repellency towards a range of liquids. In addition, the viscosity (dependent on the temperature) and the equilibrium vapor pressure of the lubricant must be such that the lubricant is compatible with the required environment. For example, if the viscosity is too high, the lubricant may not spread homogeneously on the surface. Hence, the solid surface may be exposed to the condensate, resulting in filmwise condensation. However, if the viscosity is too low, the condensate might displace the lubricant, yielding filmwise condensation as discussed above. The latter challenge could be reduced by carefully choosing the underlying solid surface as indicated in the study by Wong et al. [40]. They observed that lyophobic underlying surfaces decrease the chance of lubricant displacement.

[13] This is termed "oleophobic" by Rykaczewski et al. (2014), but exhibit $\theta_Y < 90°$

5. CO_2 Condensation on Superlyophobic Surfaces

Now, we move away from the solid science and into the landscape of conjectures. If there was little literature on superlyophobicity in general, there is, as far as we know, none on surfaces promoting dropwise condensation of CO_2. As a result, an extrapolation from the knowledge attained in the former field is necessary. First, we will compare relevant chemical and physical properties of (liquid) CO_2 with the condensates from the previous sections. Subsequently, we will try to qualitatively comment on and evaluate the performance of suggested surface morphologies (from the previous sections) using CO_2 as the condensate.

5.1. Surface tension of CO_2 compared with other liquids

Table 2 shows the surface tension of various low surface tension liquids, water and CO_2. At room temperature, CO_2 has significantly lower surface tension than the other fluids, however, the surface tension of CO_2 increases dramatically as the surrounding temperature decreases. At around $-50\,°C$, the surface tension of CO_2 is comparable to the organic liquids, shown in Table 2. By assuming that surface tension is the determining factor, and that temperature has no other influence, it is possible that previous results using e.g. pentane as the test liquid [11], may be transferable to CO_2.

Table 2: Chemical and physical properties of liquid CO_2 compared to other liquids

Liquid	**Surface Tension [$\frac{mN}{m}$]**	**Temp [°C]**
CO_2	16.54 [59]	-52.2
CO_2	1.19 [60]	20
Hexadecane	28.12 [61]	20
Pentane	~~15.86 [62]~~ 15.7 [58]	21
Hexane	18.52 [63]	20
Ethanol	22.28 [63]	20
Water	72.75 [62]	20

5.2. Candidate surfaces for promoting dropwise condensation of CO_2

In commercially available CO_2 condensers, copper and copper oxide materials are commonly used, and filmwise condensation is the default mode. To achieve dropwise condensation of CO_2, it is necessary to lower the surface energy of the copper. Functionalization of an untextured Cu surface with a fluid with low surface energy alone, is however, an unlikely path due to low durability and still too high surface energy. Nevertheless, the combination of functionalization and nano- and microscaled surface structuring has been shown to be crucial for achieving superlyophobicity [57], and is probably imperative for the case of CO_2. Regarding low surface energy chemicals, e.g. fluorinated or perfluorinated materials, it must be pointed out that the literature does not contain examples of tests done with surfaces coated with such materials in a CO_2 environment. Conduction of proper tests is therefore necessary for determining the applicability of fluorinated compounds for dropwise condensation of CO_2.

Structured surfaces already proven to yield superlyophobicity are a good starting point for achieving dropwise condensation of CO_2. The design criteria by Wu et al. [53] in Equation (12) should be fulfilled also for CO_2, and used for designing a surface that promotes CO_2 droplets in the Cassie state.

A previous review on superomniphobic surfaces pointed out the importance of a re-entrant structure for achieving superlyophobicity [57]. One such surface has been fabricated and tested by Tuteja et al. [58]. This surface has been tested for fluids with surface tension down to ~~$15.1\,\mathrm{mN\,m^{-1}}$~~ $15.7\,\mathrm{mN\,m^{-1}}$ (pentane), and is therefore a candidate for the CO_2 case. ~~However~~Liu et al. also pointed out the importance of re-entrant surfaces [64]. For achieving droplets in the Cassie state for liquids of very low surface tension, even for fluorinated compounds (C_6F_{14}, $\gamma = 10\,\mathrm{mN\,m^{-1}}$), a doubly re-entrant structure is required. However, Wu and Tuteja used fluorinated chemicals to achieve lyophobicity, and the applicability of fluorine chemicals in a CO_2 environment ~~, and~~ is unknown. In addition, the low temperature durability of the surface ~~, are~~ is unknown, and therefore ~~important issues~~ an important issue to address. ~~In addition~~Also, neither of the surfaces by Wu et al.~~or~~ , Tuteja et al. or Liu et al. are tested with

condensing vapor, so the direct applicability to dropwise condensation of CO_2 is unknown. The re-entrant surfaces, both single and double, have no defence against internal condensation within the structures [64], and a Wenzel-to-Cassie transition is not expected.

On the other hand, Rykaczewski et al. determined the condensation mode for seven different low surface tension fluids and water, on three different surfaces, in which one is a SLIPS [11]. Even though the contact angle towards the tested organic oils were less than 90° for all surfaces, the condensation occurred in the dropwise mode for several of the liquids. Special attention should be given to the condensation of pentane, which condensed in the dropwise mode on two of the three tested surfaces, even though the surface tension is only ~~$15.1\,\mathrm{mN\,m^{-1}}$~~ $15.7\,\mathrm{mN\,m^{-1}}$. It should also be noted that perfluorohexane with a surface tension of $12\,\mathrm{mN\,m^{-1}}$ condensed in the filmwise mode for all surfaces, which indicates a limit as to how low the surface tension can be to achieve dropwise condensation on this kind of surfaces. In any case, the flat oleophobic surfaces and the SLIPS surface fabricated in this work are candidates for dropwise condensation of CO_2.

For using SLIPS as a surface for condensation, the surface tension of CO_2 is again an issue, and the experiments have to be performed at low temperatures. The requirement for low temperature introduces yet another challenge: The ability of the surface and the infusion liquid to endure extreme conditions. Thermal compression resulting in material cracking and failure is only one example. Decomposition and/or freezing of the lubricant is another. However, low temperatures do not necessarily cause low mechanical robustness, as shown by Wang et al. [65]. They tested three different liquids for SLIPSs for anti-icing applications, and found that the superhydrophobicity was maintained, but reduced, down to $-20\,^{\circ}\mathrm{C}$ for one of the lubricants. The reduction in superhydrophobicity comes from increased pinning of water droplets on the surface, which could also be the case for CO_2 droplets. The work by Lu et al. [66] resulted in a non-wetting SLIPS against water and various liquids, such as coffee and cooking oils, also after thermal tests with liquid nitrogen ($-196\,^{\circ}\mathrm{C}$). These

results are promising for low temperature condensation of CO_2 , but as for most of the results in the literature, this work is also a test of non-wetting behaviour, not for promotion of dropwise condensation. Even though superlyophobicity is necessary for dropwise condensation, it is not the only requirement, and tests with condensing vapor must be conducted at different thermal conditions.

Generally, SLIPS are promising candidates for CO_2 condensation. However, care should be taken to choose the proper lubricant. As said above, temperature stability is important. Even more crucial is the immiscibility of the lubricant towards CO_2. If CO_2 is miscible with the lubricant it would displace the lubricant, and flood the underlying surface. Lubricants that are immiscible for low surface tension fluids can be found by utilizing the model set forth by Preston et al [45]. For CO_2 it will not be easy to find a suitable lubricant. Liquid CO_2 is a good solvent for several oily substances that are often used as lubricants for SLIPS repelling water.

CO_2 in its supercritical form is a superior solvent and even though liquid and supercritical CO_2 does not have equal behavior, this property will pose a challenge when condenser surfaces are coated with chemicals. This is the case both for SLIPS and for surfaces where fluorinated compounds are used for lowering the surface energy. This challenge has not been addressed previously, and work has to be done on the matter.

6. Summary and ideas for further work

Through this literature review it is shown that comprehensive design criteria for superhydrophobic surfaces have been developed, and that different sets of criteria by different research groups, are consistent. Most of the work done is applicable to static water droplets and the non-wetting behaviour of rough surfaces. Less work is conducted on condensing water droplets, and even less on condensing low surface tension liquids. Nevertheless, the previous work on superlyophobic surfaces indicate that re-entrant surfaces with structures with at least two length scales (hierarchical structures) that are coated with a low

surface energy fluid such as a silane, is likely to yield superlyophobicity, i.e. non-wetting behaviour towards all liquids, including CO_2. Examples of surface designs that could be combined to give the above described surface are those by Rykasczewski et al. [11], Wu et al. [53], and Tuteja et al. [52], with the basic design criteria of Sarkar et al. [18] as a basis.

Even with the design criteria at hand, there are still important parameters of liquid CO_2 that is not known. One very important parameter for using the design criteria is the equilibrium contact angle of the liquid on the surface. This parameter is not known for CO_2 liquid in a CO_2 vapor environment, and a necessary starting point for future work is therefore to measure the contact angle of a CO_2 droplet on a flat surface. It is also necessary to test various low surface energy chemicals, such as fluorines, for compatibility with CO_2. The low temperature behaviour and immiscibility of candidate lubricants towards CO_2 for fabrication of SLIPS are other parameters to be tested.

Acknowledgements

This publication has been produced with the support of the Research Council of Norway through the CLIMIT funding program (254813/E20).

References

[1] K. Chua, S. Chou, W. Yang, J. Yan, Achieving better energy-efficient air conditioning – a review of technologies and strategies, Applied Energy 104 (2013) 87 – 104. doi:https://doi.org/10.1016/j.apenergy.2012.10.037.
URL http://www.sciencedirect.com/science/article/pii/S030626191200743X

[2] J. Beér, Combustion technology developments in power generation in response to environmental challenges, Progress in Energy and Combustion Science 26 (4) (2000) 301 – 327. doi:https:

//doi.org/10.1016/S0360-1285(00)00007-1.

URL http://www.sciencedirect.com/science/article/pii/S0360128500000071

[3] E. Brendeng, J. Hetland, State of the art in liquefaction technologies for natural gas, in: J. Hetland, T. Gochitashvili (Eds.), Security of Natural Gas Supply through Transit Countries. NATO Science Series II: Mathematics, Physics and Chemistry, Vol. 149, Springer, 2004, pp. 75–102. doi:10.1007/1-4020-2078-3_5.

[4] D. Berstad, P. Nekså, R. Anantharaman, Low-temperature co2 removal from natural gas, Energy Procedia 26 (2012) 41 – 48, 2nd Trondheim Gas Technology Conference. doi:https://doi.org/10.1016/j.egypro.2012.06.008.

URL http://www.sciencedirect.com/science/article/pii/S187661021201048X

[5] A. Aspelund, M. Molnvik, G. D. Koeijer, Ship transport of CO2, Chemical Engineering Research and Design 84 (9) (2006) 847 – 855. doi:http://dx.doi.org/10.1205/cherd.5147.

URL http://www.sciencedirect.com/science/article/pii/S0263876206729665

[6] P. B. Weisensee, N. K. Neelakantan, K. S. Suslick, A. M. Jacobi, W. P. King, Impact of air and water vapor environments on the hydrophobicity of surfaces, Journal of Colloid and Interface Science 453 (2015) 177–185. doi:10.1016/j.jcis.2015.04.060.

URL http://www.sciencedirect.com/science/article/pii/S0021979715004373

[7] X. Ma, J. W. Rose, D. Xu, J. Lin, B. Wang, Advances in dropwise condensation heat transfer: Chinese research, Chemical Engineering Journal 78 (2-3) (2000) 87–93. doi:10.1016/S1385-8947(00)00155-8.

URL http://www.sciencedirect.com/science/article/pii/S1385894700001558

[8] B. S. Sikarwar, N. K. Battoo, S. Khandekar, K. Muralidhar, Dropwise condensation underneath chemically textured surfaces: Simulation and experiments, Journal of Heat Transfer 133 (2) (2010) 021501–021501. doi:10.1115/1.4002396.
URL http://dx.doi.org/10.1115/1.4002396

[9] J. B. Boreyko, C.-H. Chen, Self-propelled dropwise condensate on superhydrophobic surfaces, Physical Review Letters 103 (18) (2009) 184501. doi:10.1103/PhysRevLett.103.184501.
URL http://link.aps.org/doi/10.1103/PhysRevLett.103.184501

[10] A. Milionis, I. S. Bayer, E. Loth, Recent advances in oil-repellent surfaces, International Materials Reviews 61 (2) (2016) 101–126. doi:10.1080/09506608.2015.1116492.
URL http://dx.doi.org/10.1080/09506608.2015.1116492

[11] K. Rykaczewski, A. T. Paxson, M. Staymates, M. L. Walker, X. Sun, S. Anand, S. Srinivasan, G. H. McKinley, J. Chinn, J. H. J. Scott, K. K. Varanasi, Dropwise condensation of low surface tension fluids on omniphobic surfaces, Scientific Reports 4. doi:10.1038/srep04158.
URL http://www.nature.com/articles/srep04158

[12] P. C. Hiemenz, R. Rajagopalan, Principles of Colloid and Surface Chemistry, 3rd Edition, CRC Press, 1997.

[13] D. Quéré, Wetting and roughness, Annual Review of Materials Research 38 (1) (2008) 71–99. doi:10.1146/annurev.matsci.38.060407.132434.
URL http://dx.doi.org/10.1146/annurev.matsci.38.060407.132434

[14] P. Mazumder, Y. Jiang, D. Baker, A. Carrilero, D. Tulli, D. Infante, A. T. Hunt, V. Pruneri, Superomniphobic, transparent, and antireflection surfaces based on hierarchical nanostructures, Nano Letters 14 (8) (2014)

4677–4681. doi:10.1021/nl501767j.
URL http://dx.doi.org/10.1021/nl501767j

[15] C. Dorrer, J. Rühe, Some thoughts on superhydrophobic wetting, Soft Matter 5 (1) (2008) 51–61. doi:10.1039/B811945G.
URL http://pubs.rsc.org/en/content/articlelanding/2009/sm/b811945g

[16] C.-W. Lo, C.-C. Wang, M.-C. Lu, Scale effect on dropwise condensation on superhydrophobic surfaces, ACS Applied Materials & Interfaces 6 (16) (2014) 14353–14359. doi:10.1021/am503629f.
URL http://dx.doi.org/10.1021/am503629f

[17] M. E. Kavousanakis, N. T. Chamakos, A. G. Papathanasiou, Connection of intrinsic wettability and surface topography with the apparent wetting behavior and adhesion properties, The Journal of Physical Chemistry C 119 (27) (2015) 15056–15066. doi:10.1021/acs.jpcc.5b00718.
URL http://dx.doi.org/10.1021/acs.jpcc.5b00718

[18] A. Sarkar, A.-M. Kietzig, Design of a robust superhydrophobic surface: thermodynamic and kinetic analysis, Soft Matter 11 (10) (2015) 1998–2007. doi:10.1039/C4SM02787F.
URL http://pubs.rsc.org/en/content/articlelanding/2015/sm/c4sm02787f

[19] A. Sarkar, A.-M. Kietzig, General equation of wettability: A tool to calculate the contact angle for a rough surface, Chemical Physics Letters 574 (2013) 106–111. doi:10.1016/j.cplett.2013.04.055.
URL http://www.sciencedirect.com/science/article/pii/S0009261413005678

[20] Q.-S. Zheng, Y. Yu, Z.-H. Zhao, Effects of hydraulic pressure on the stability and transition of wetting modes of superhydrophobic surfaces, Langmuir 21 (26) (2005) 12207–12212. doi:10.1021/la052054y.
URL http://dx.doi.org/10.1021/la052054y

[21] J. Drelich, J. D. Miller, R. J. Good, The effect of drop (bubble) size on advancing and receding contact angles for heterogeneous and rough solid surfaces as observed with sessile-drop and captive-bubble techniques, Journal of Colloid and Interface Science 179 (1) (1996) 37–50. doi:10.1006/jcis.1996.0186.
URL http://linkinghub.elsevier.com/retrieve/pii/S0021979796901861

[22] B. P. Lloyd, P. N. Bartlett, R. J. K. Wood, Wetting of surfaces made of hydrophobic cavities, Langmuir 31 (34) (2015) 9325–9330. doi:10.1021/acs.langmuir.5b02107.
URL http://dx.doi.org/10.1021/acs.langmuir.5b02107

[23] B. Haimov, S. Pechook, O. Ternyak, B. Pokroy, Shape of water-air interface beneath a drop on a superhydrophobic surface revealed: Constant curvature that approaches zero, The Journal of Physical Chemistry C 117 (13) (2013) 6658–6663. doi:10.1021/jp312650f.
URL http://dx.doi.org/10.1021/jp312650f

[24] M. Nosonovsky, B. Bhushan, Superhydrophobic surfaces and emerging applications: Non-adhesion, energy, green engineering, Current Opinion in Colloid & Interface Science 14 (4) (2009) 270–280. doi:10.1016/j.cocis.2009.05.004.
URL http://www.sciencedirect.com/science/article/pii/S1359029409000399

[25] R. Hensel, A. Finn, R. Helbig, S. Killge, H.-G. Braun, C. Werner, In situ experiments to reveal the role of surface feature sidewalls in the cassie-wenzel transition, Langmuir 30 (50) (2014) 15162–15170. doi:10.1021/la503601u.
URL http://dx.doi.org/10.1021/la503601u

[26] R. Enright, N. Miljkovic, A. Al-Obeidi, C. V. Thompson, E. N. Wang, Condensation on superhydrophobic surfaces: The role of local energy bar-

riers and structure length scale, Langmuir 28 (40) (2012) 14424–14432. doi:10.1021/la302599n.
URL http://dx.doi.org/10.1021/la302599n

[27] C.-W. Lo, C.-C. Wang, M.-C. Lu, Spatial control of heterogeneous nucleation on the superhydrophobic nanowire array, Advanced Functional Materials 24 (9) (2014) 1211–1217. doi:10.1002/adfm.201301984.
URL http://onlinelibrary.wiley.com/doi/10.1002/adfm.201301984/abstract

[28] M. Nosonovsky, B. Bhushan, Biomimetic superhydrophobic surfaces: Multiscale approach, Nano Letters 7 (9) (2007) 2633–2637. doi:10.1021/nl071023f.
URL http://dx.doi.org/10.1021/nl071023f

[29] R. Narhe, Water condensation on ultrahydrophobic flexible micro pillar surface, Europhysics Letters 114 (3) (2016) 36002. doi:10.1209/0295-5075/114/36002.
URL http://stacks.iop.org/0295-5075/114/i=3/a=36002

[30] J. Zhu, Y. Luo, J. Tian, J. Li, X. Gao, Clustered ribbed-nanoneedle structured copper surfaces with high-efficiency dropwise condensation heat transfer performance, ACS Applied Materials & Interfaces 7 (20) (2015) 10660–10665. doi:10.1021/acsami.5b02376.
URL http://dx.doi.org/10.1021/acsami.5b02376

[31] Z. He, J. He, Z. Zhang, Selective growth of metallic nanostructures on microstructured copper substrate in solution, CrystEngComm 17 (2015) 7262–7269. doi:10.1039/c5ce01093d.

[32] D. M. Anderson, M. K. Gupta, A. A. Voevodin, C. N. Hunter, S. A. Putnam, V. V. Tsukruk, A. G. Fedorov, Using amphiphilic nanostructures to enable long-range ensemble coalescence and surface rejuvenation in dropwise condensation, ACS Nano 6 (4) (2012) 3262–3268. doi:

10.1021/nn300183d.
URL http://dx.doi.org/10.1021/nn300183d

[33] X. Chen, J. Wu, R. Ma, M. Hua, N. Koratkar, S. Yao, Z. Wang, Nanograssed micropyramidal architectures for continuous dropwise condensation, Advanced Functional Materials 21 (24) (2011) 4617–4623. doi:10.1002/adfm.201101302.
URL http://onlinelibrary.wiley.com/doi/10.1002/adfm.201101302/abstract

[34] N. Miljkovic, R. Enright, Y. Nam, K. Lopez, N. Dou, J. Sack, E. N. Wang, Jumping-droplet-enhanced condensation on scalable superhydrophobic nanostructured surfaces, Nano Letters 13 (1) (2013) 179–187. doi:10.1021/nl303835d.
URL http://dx.doi.org/10.1021/nl303835d

[35] H. Kim, Y. Nam, Condensation behaviors and resulting heat transfer performance of nano-engineered copper surfaces, International Journal of Heat and Mass Transfer 93 (2016) 286–292. doi:10.1016/j.ijheatmasstransfer.2015.09.079.
URL http://www.sciencedirect.com/science/article/pii/S0017931015300351

[36] R. Enright, N. Miljkovic, J. Sprittles, K. Nolan, R. Mitchell, E. N. Wang, How coalescing droplets jump, ACS Nano 8 (10) (2014) 10352–10362. doi:10.1021/nn503643m.
URL http://dx.doi.org/10.1021/nn503643m

[37] N. Miljkovic, D. J. Preston, R. Enright, E. N. Wang, Electric-field-enhanced condensation on superhydrophobic nanostructured surfaces, ACS Nano 7 (12) (2013) 11043–11054. doi:10.1021/nn404707j.
URL http://pubs.acs.org/doi/abs/10.1021/nn404707j

[38] D. Torresin, M. K. Tiwari, D. Del Col, D. Poulikakos, Flow condensation on copper-based nanotextured superhydrophobic surfaces, Langmuir 29 (2)

(2013) 840–848. doi:10.1021/la304389s.
URL http://dx.doi.org/10.1021/la304389s

[39] Z. He, Z. Zhang, J. He, Cuo/Cu based superhydrophobic and self-cleaning surfaces, Scripta Materiala 118 (2016) 60–64. doi:10.1016/j.scriptamat.2016.03.015.
URL http://www.sciencedirect.com/science/article/pii/S1359646216300884

[40] T.-S. Wong, S. H. Kang, S. K. Y. Tang, E. J. Smythe, B. D. Hatton, A. Grinthal, J. Aizenberg, Bioinspired self-repairing slippery surfaces with pressure-stable omniphobicity, Nature 477 (7365) (2011) 443–447. doi:10.1038/nature10447.
URL http://www.nature.com/nature/journal/v477/n7365/full/nature10447.html

[41] T. Kajiya, F. Schellenberger, P. Papadopoulos, D. Vollmer, H.-J. Butt, 3d imaging of water-drop condensation on hydrophobic and hydrophilic lubricant-impregnated surfaces, Scientific Reports 6 (2016) 23687. doi:10.1038/srep23687.
URL http://www.nature.com/articles/srep23687

[42] K. Chen, Y. Wu, S. Zhou, L. Wu, Recent development of durable and self-healing surfaces with special wettability, Macromolecular Rapid Communications 37 (6) (2016) 463–485. doi:10.1002/marc.201500591.
URL http://onlinelibrary.wiley.com/doi/10.1002/marc.201500591/abstract

[43] X. Dai, B. B. Stogin, S. Yang, T.-S. Wong, Slippery wenzel state, ACS Nano 9 (9) (2015) 9260–9267. doi:10.1021/acsnano.5b04151.
URL http://dx.doi.org/10.1021/acsnano.5b04151

[44] R. Xiao, N. Miljkovic, R. Enright, E. N. Wang, Immersion condensation on oil-infused heterogeneous surfaces for enhanced heat transfer, Scientific

Reports 3. doi:10.1038/srep01988.
URL http://www.nature.com/articles/srep01988

[45] D. J. Preston, Y. Song, Z. Lu, D. S. Antao, E. N. Wang, Design of lubricant infused surfaces, ACS Applied Materials & Interfaces 9 (48) (2017) 42383–42392. doi:10.1021/acsami.7b14311.
URL http://dx.doi.org/10.1021/acsami.7b14311

[46] S. Anand, A. T. Paxson, R. Dhiman, J. D. Smith, K. K. Varanasi, Enhanced condensation on lubricant-impregnated nanotextured surfaces, ACS Nano 6 (11) (2012) 10122–10129. doi:10.1021/nn303867y.
URL http://dx.doi.org/10.1021/nn303867y

[47] P. B. Weisensee, Y. Wang, Q. Hongliang, D. Schultz, W. P. King, N. Miljkovic, Condensate droplet size distribution on lubricant-infused surfaces, International Journal of Heat and Mass Transfer 109 (2017) 187 – 199. doi:https://doi.org/10.1016/j.ijheatmasstransfer.2017.01.119.
URL http://www.sciencedirect.com/science/article/pii/S0017931016334925

[48] S. Kim, K. J. Kim, Dropwise condensation modeling suitable for superhydrophobic surfaces, Journal of Heat Transfer 133 (2011) 081502–1 – 081502–8. doi:10.1115/1.4003742.
URL http://heattransfer.asmedigitalcollection.asme.org/article.aspx?articleid=1449979

[49] N. Miljkovic, R. Enright, E. N. Wang, Effect of droplet morphology on growth dynamics and heat transfer during condensation on superhydrophobic nanostructured surfaces, ACS NANO 6 (2) (2012) 1776–1785. doi:10.1021/nn205052a.
URL http://pubs.acs.org/doi/abs/10.1021/nn205052a

[50] A. Ghosh, S. Beaini, B. J. Zhang, R. Ganguly, C. M. Megaridis, Enhancing dropwise condensation through bioinspired wettability patterning, Lang-

muir 30 (43) (2014) 13103–13115. doi:10.1021/la5028866.
URL https://doi.org/10.1021/la5028866

[51] P. S. Mahapatra, A. Ghosh, R. Ganguly, C. M. Megaridis, Key design and operating parameters for enhancing dropwise condensation through wettability patterning, International Journal of Heat and Mass Transfer 92 (2016) 877–883. doi:10.1016/j.ijheatmasstransfer.2015.08.106.
URL http://www.sciencedirect.com/science/article/pii/S0017931015307158

[52] A. Tuteja, W. Choi, M. Ma, J. M. Mabry, S. A. Mazzella, G. C. Rutledge, G. H. McKinley, R. E. Cohen, Designing superoleophobic surfaces, Science 318 (5856) (2007) 1618–1622. doi:10.1126/science.1148326.
URL http://science.sciencemag.org/content/318/5856/1618

[53] T. Wu, Y. Suzuki, Design, microfabrication and evaluation of robust high-performance superlyophobic surfaces, Sensors and Actuators B: Chemical 156 (1) (2011) 401–409. doi:10.1016/j.snb.2011.04.065.
URL http://www.sciencedirect.com/science/article/pii/S0925400511003625

[54] C. W. Extrand, Model for contact angles and hysteresis on rough and ultraphobic surfaces, Langmuir 18 (21) (2002) 7991–7999. doi:10.1021/la025769z.
URL http://dx.doi.org/10.1021/la025769z

[55] W. Choi, A. Tuteja, J. M. Mabry, R. E. Cohen, G. H. McKinley, A modified cassie–baxter relationship to explain contact angle hysteresis and anisotropy on non-wetting textured surfaces, Journal of Colloid and Interface Science 339 (1) (2009) 208–216. doi:10.1016/j.jcis.2009.07.027.
URL http://www.sciencedirect.com/science/article/pii/S0021979709009576

[56] X. Deng, L. Mammen, H.-J. Butt, D. Vollmer, Candle soot as a template for a transparent robust superamphiphobic coating, Science 335 (6064) (2012)

67–70. doi:10.1126/science.1207115.
URL http://science.sciencemag.org/content/335/6064/67

[57] A. K. Kota, G. Kwon, A. Tuteja, The design and applications of superomniphobic surfaces, NPG Asia Materials 6 (7) (2014) e109. doi:10.1038/am.2014.34.
URL http://www.nature.com/am/journal/v6/n7/full/am201434a.html

[58] A. Tuteja, W. Choi, J. M. Mabry, G. H. McKinley, R. E. Cohen, Robust omniphobic surfaces, Proceedings of the National Academy of Sciences 105 (47) (2008) 18200–18205. doi:10.1073/pnas.0804872105.
URL http://www.pnas.org/content/105/47/18200.full.pdf

[59] E. L. Quinn, The surface tension of liquid carbon dioxide, Journal of the American Chemical Society 49 (11) (1927) 2704–2711. doi:10.1021/ja01410a006.
URL http://dx.doi.org/10.1021/ja01410a006

[60] B. M. Fronk, S. Garimella, Condensation of carbon dioxide in microchannels, International Journal of Heat and Mass Transfer 100 (2016) 150 – 164. doi:http://dx.doi.org/10.1016/j.ijheatmasstransfer.2016.03.083.
URL http://www.sciencedirect.com/science/article/pii/S0017931015314162

[61] L. I. Rolo, A. I. Caco, A. J. Queimada, I. M. Marrucho, J. A. P. Coutinho, Surface tension of heptane, decane, hexadecane, eicosane, and some of their binary mixtures, Journal of Chemical & Engineering Data 47 (6) (2002) 1442–1445. doi:10.1021/je025536+.
URL http://dx.doi.org/10.1021/je025536+

[62] N. B. Vargaftik, B. N. Volkov, L. D. Voljak, International tables of the surface tension of water, Journal of Physical and Chemical Reference Data

12 (3) (1983) 817–820. doi:10.1063/1.555688.
URL http://dx.doi.org/10.1063/1.555688

[63] B. Giner, A. Villares, S. Martin, H. Artigas, C. Lafuente, Study of the temperature dependence of surface tensions of some alkanol + hexane mixtures, Journal of Chemical & Engineering Data 52 (5) (2007) 1904–1907. doi:10.1021/je700215z.
URL http://dx.doi.org/10.1021/je700215z

[64] T. ". Liu, C.-J. ". Kim, Turning a surface superrepellent even to completely wetting liquids, Science 346 (6213) (2014) 1096–1100. arXiv:http://science.sciencemag.org/content/346/6213/1096.full.pdf, doi:10.1126/science.1254787.
URL http://science.sciencemag.org/content/346/6213/1096

[65] N. Wang, D. Xiong, S. Pan, K. Wang, Y. Shi, Y. Deng, Robust superhydrophobic coating and the anti-icing properties of its lubricants-infused-composite surface under condensing condition, New Journal of Chemistry 41 (2017) 1846–1853. doi:10.1039/C6NJ02824A.
URL http://dx.doi.org/10.1039/C6NJ02824A

[66] Y. Lu, G. He, C. J. Carmalt, I. P. Parkin, Synthesis and characterization of omniphobic surfaces with thermal, mechanical and chemical stability, RSC Adv. 6 (2016) 106491–106499. doi:10.1039/C6RA20392B.
URL http://dx.doi.org/10.1039/C6RA20392B